Journal of
Mechanics of
Materials and Structures

SINGLE MEMBER ACTUATION OF KAGOME LATTICE STRUCTURES

Anthony C. H. Leung and Simon D. Guest

Volume 2, Nº 2 February 2007

mathematical sciences publishers

JOURNAL OF MECHANICS OF MATERIALS AND STRUCTURES
Vol. 2, No. 2, 2007

SINGLE MEMBER ACTUATION OF KAGOME LATTICE STRUCTURES

ANTHONY C. H. LEUNG AND SIMON D. GUEST

The two-dimensional kagome lattice has been shown to be a promising basis for active shape-changing structures, having both low actuation resistance and high passive stiffness. Activation of some members results in a global macroscopic shape change. Small deformation models show that the kagome lattice's properties are critically dependent on its initial geometry. This paper investigates the fundamental actuation properties of a kagome lattice subject to single-member actuation, particularly when geometric nonlinearity is introduced with large actuation strains. Actuation resistance is found to be lowered with expansive actuation; a limiting peak actuation stiffness is observed when the actuator is flexible. Conversely, actuation resistance is found to increase with contractile actuation.

1. Introduction

Recent studies have shown the two-dimensional kagome lattice, shown in Figure 1, to be a prime candidate to form the backbone of *active* structures [Santos e Lucato et al. 2004; Hutchinson et al. 2003; Symons et al. 2005a; 2005b]. If linear actuators replace some members of the truss, significant global macroscopic shape changes can be achieved with a relatively small number of actuators. In order to obtain a deeper understanding of the response of the kagome lattice to actuation, this paper investigates a simple case, where an infinite kagome lattice is activated by a single actuator.

Active structures, also known as *adaptive* or *smart* structures, change their configuration, shape or other properties to better carry the type and magnitude of its design loads. Shape changes in active

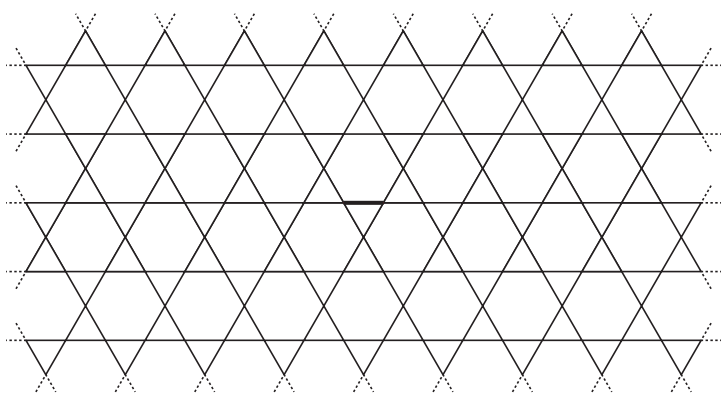

Figure 1. Part of an infinite kagome lattice. The thick line at the centre represents a single actuator.

Keywords: kagome lattice, morphing, actuation.

structures are achieved by actuation of some parts of the structure. To date, actuators manufactured are predominantly one-dimensional, where their capabilities are confined to extending and contracting along or rotating about one axis; *active truss structures* provide a way of incorporating linear actuators into a structure. The paper will focus on the structural response of the truss rather than methods of actuation; possible actuators are described in [Santos e Lucato et al. 2004; Symons et al. 2005a; 2005b].

Hutchinson et al. [2003] has shown that the planar kagome lattice can be actuated with minimal internal resistance while maintaining overall stiffness. The rigid-jointed planar kagome lattice exhibits high passive stiffness, while having a low actuation resistance. These properties are 'inherited' from the pin-jointed 'parent' [Deshpande et al. 2001], where the kagome truss is composed of rigid triangulated unit-cells, with mechanisms allowing relative motion of the cells; as member stockiness, s, is reduced, the properties of the rigid-jointed structure approaches the properties of the pin-jointed structure. The stockiness is a nondimensional measure of the aspect ratio of each member, defined as $s = k/L$, where k is the in-plane radius of gyration of each member and L is the length of the member (s is the reciprocal of the common mechanics parameter *slenderness*).

Wicks and Guest [2004] have shown, using various *linear* finite element and analytic models, that the exceptional behaviour of the kagome lattice depends on both flexure of members, and axial contraction of the bars colinear with the actuator. However, this behaviour depends crucially on the geometry of the lattice, and hence kagome lattices subjected to large actuation will be prone to *geometrically nonlinear* effects.

This paper investigates geometric nonlinearity in the single-bar actuation behaviour of kagome lattices with stockiness ranging from 0.001 to 0.05 (an areal density of $\simeq 0.3\% \rightarrow 15\%$), covering the likely range of practical interest, with actuation strains of up to $\pm 50\%$. The two experimental active kagome lattice structures described in the literature have $s = 0.007$ [Santos e Lucato et al. 2004] and $s \simeq 0.0085$ [Symons et al. 2005a; 2005b].

The paper is structured as follows. Section 2 will describe the computational model used in the finite element analyses. Section 3 will describe the deformed mode shapes of the lattice following actuation, and Section 4 will investigate the build-up of force in the actuator. Section 5 explores the actuation limit due to material yield and member buckling. Section 6 provides a discussion of the results.

2. Computational model

The planar kagome lattice is a class of *repetitive truss* structure. Noor [1998] reviewed analysis methods for repetitive trusses and described the following four classes of approach, with increasing computational expense:

(1) The substitute continuum approach which the truss considered is replaced by a continuum with resembling structural properties [Timoshenko and Gere 1961].

(2) The periodic structure approach, which employs a transfer matrix relating a state vector on the boundaries of the unit cell [Noor and Zhang 2006].

(3) The direct field method, which uses finite difference equations on unit cells [Dean 1976; Renton 1984].

(4) The direct or finite element method, which discretizes the entire structure [Akin 1986].

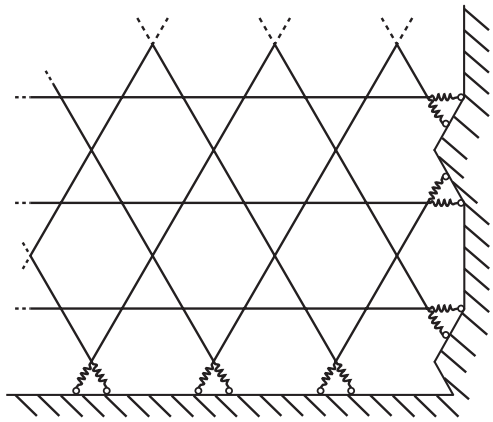

Figure 2. The spring boundary condition; boundary nodes of the kagome lattice are connected to spring elements to simulate the response of an infinite grid.

or a combination of the above [Karpov et al. 2002]. This paper uses the finite element method as the basis of its analyses. Computational time has been substantially reduced by the use of symmetry and an elastic boundary conditions to mimic infinity, making the entire array of result from FEM feasible.

The finite element package ABAQUS was used to model the structure in two and three dimensions. The model used was designed to represent an infinite lattice: to do this a finite rectangular lattice, with a width 80 times the individual member length L, and a height of $30 \times L\sqrt{3}/2 \approx 26L$, was used together with a spring boundary condition, as shown in Figure 2. The derivation of the required spring stiffness to represent the rest of an infinite lattice is given in the Appendix by assuming linearity, and decoupling between different boundary points; the required stiffness turns out to be proportional to the stockiness, s. Computational effort is reduced by the assumption that the response is symmetric about the central vertical line.

Two extreme cases are considered for the stiffness of the actuator: either that the actuator has the same elastic properties as every other bar, which we refer to as the 'flexible' actuator; or the actuator is a pin-jointed infinitely stiff bar that imposes a fixed distance between its ends, which we refer to as the 'stiff' actuator. Apart from the actuator, all other bars in the lattice have identical properties. The actuator is either axially elongated, defined here as positive actuation, or contracted, defined here as negative actuation. Flexible actuation is achieved by raising or lowering the overall temperature in the system and using an actuator that has a coefficient of thermal expansion of unity, while the rest of the structure has a coefficient of thermal expansion of zero. Stiff actuation is achieved by increasing or decreasing the distance between the two ends of the actuator.

Each bar of the lattice except the actuator is modelled with four 3-noded Timoshenko (shear flexible) beam elements; the flexible actuator is modelled with eight such elements, while the rigid actuator is modelled by imposing a relative displacement. Test cases showed that using a higher number of elements per bar gave results that were indistinguishable from those reported here. No consideration is given to the actual size of a joint between bars, which is assumed to be at a point. For most analyses, each bar has a circular cross-section of radius r. The material properties are assumed to remain linear, with a Young's modulus E, giving an axial stiffness AE, where $A = \pi r^2$, and flexural stiffness EI, where

$I = Ak^2 = Ar^2/4$; $k = r/2$ for a round bar. Bars with rectangular cross-sections are used for out-of-plane buckling analyses, with area $A = bd$, where b and d are out-of-plane and in-plane dimensions respectively. Similarly, this gives axial and in-plane flexural stiffness AE and $EI = EAk^2$, but with $k = d/2\sqrt{3}$.

Lattices were considered with stockiness s ranging from 0.001 to 0.05, which covers the range likely to be of interest for application. We describe the actuation in terms of an *actuation strain*, ε_a: we define this strain to be the extension the bar would experience if unconstrained, divided by its original length; it is defined as being positive when the bar gets longer. The actual strain experienced in the flexible actuator, ε, is smaller than the actuation strain, as the rest of the structure imposes an axial force F to the actuator, which this gives rise to an elastic strain of opposite sign to ε_a. With a stiff actuator, the actuation strain equals the elastic strain: $\varepsilon = \varepsilon_a$.

3. Mode of deformation

This section will separately present the shape of the deformed lattice following expansive and contractile actuations. In each case, the geometrically nonlinear results for both the stiff and flexible actuator are compared with the results of a linear model. The comparisons are done for an actuation strain of $\pm 50\%$, and for three different values of stockiness. It is assumed that the grid has no imperfection, and only in-plane deformation are considered — Section 5.3 will revisit these assumptions.

The mode of deformation for a linear calculation was characterized by Wicks and Guest [2004]; essentially identical results are presented here for the linear case. The key features of the linear deformation mode can be observed in the results shown in the middle panels of Figure 3, top and bottom. Deformation is confined largely to a corridor parallel with the actuator. The deformation dies away in an approximately exponential manner, and the rate of decay is proportional to the stockiness, s. The linear results provide a useful base to compare the geometrically nonlinear results in the left and right panels of Figure 3 (top and bottom).

3.1. ***Nonlinear actuation: expansion.*** A key feature of the linear response is that lengthening of the actuator can only be achieved by shortening the other members in line with the actuators, leading to the interesting combined bending and stretching responses observed in [Wicks and Guest 2004], with an exponential decay in deformation with distance from the actuator. However, once the initial straight lines of bars has been bent by actuation, further shortening can occur by bending alone.

The deformed shape of the lattice calculated using the geometrically nonlinear model, for $\varepsilon_a = 50\%$, is shown in Figure 3, top left, for the flexible actuator, and Figure 3, top right, for the stiff actuator. Both sets of results show increased localisation of the deformation when compared with the linear calculation shown in Figure 3, top middle, and this increased localisation is greater for smaller stockiness s (but note that the linear results themselves show *less* localisation as s is decreased). The key observation, however, is that for the flexible actuator, the deformation is almost entirely localised in the actuator itself.

3.2. ***Nonlinear actuation: contraction.*** As for expansion, in the linear regime, the shortening of the actuator can only be achieved by lengthening of the other members in line with the actuator. However, unlike during actuator expansion, bending of these bars due to actuation does not then make deformation of other members in line with the actuator any easier.

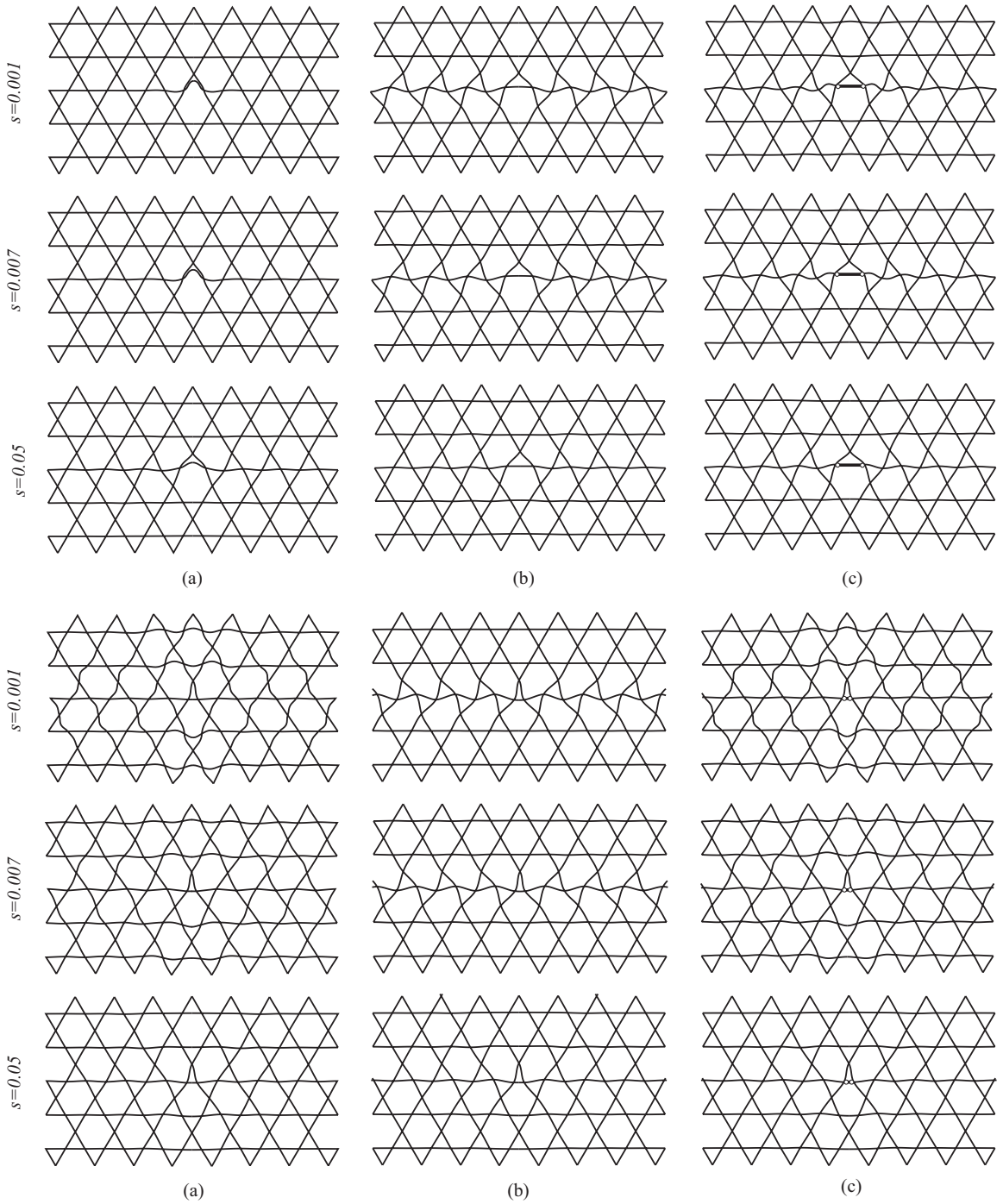

Figure 3. Deformed kagome lattices under positive actuation for $\varepsilon_a = 0.5$ (top) and negative actuation for $\varepsilon_a = -0.5$ (bottom), as well as different values of bar stockiness: (a) nonlinear actuation with a flexible actuator, (b) linear calculation and (c) nonlinear actuation with a stiff actuator.

The deformed shape of the lattice calculated using the geometrically nonlinear model, for $\varepsilon_a = -50\%$, is shown in Figure 3, bottom left, for the flexible actuator, and Figure 3, bottom right, for the stiff actuator. The linear calculation results shown in Figure 3, bottom middle, are identical to the expansion case but with a sign change for deformation.

Both sets of geometrically nonlinear results show decreasing localisation as stockiness is reduced. In the linear case, deformation is primarily confined within the corridor of bars colinear to the actuated member; but in the geometrically nonlinear cases the deformation spreads to neighbouring corridors. Unlike the expansion case, the results appear almost identical for the stiff and flexible actuators.

4. Actuation forces

This section will describe the force, F (defined as compression positive), developed in the actuator as it is activated. For small deformations, when the bar is approximately straight, F is nearly constant along the length of the actuated bar; for larger deformations we define F to be an average of the varying force along the bar.

A nondimensional form of the force can be defined by comparing the force with that required to stretch a bar: this formulation was implicit in [Wicks and Guest 2004] and explicit in [Leung et al. 2004]. For consistency, we will retain this formulation, and define

$$\hat{F} = \frac{F}{EA}$$

where EA is the axial stiffness of the actuator.

Figure 4 shows a plot of actuation force against actuation strain for three values of stockiness, for both the stiff and flexible actuator. In all cases, the plots show a softening response to expansion of the actuator (+ve ε_a), and a stiffening response to contraction ($-$ve ε_a). For expansion of the actuator the results for the flexible actuator clearly show greater softening. In fact, in all three plots the actuation force $\hat{F}$ reaches a peak, but this can only be clearly seen in Figure 4 for $s = 0.05$, where $\hat{F}$ reaches a peak at $\varepsilon_a = 40\%$. For the stiff actuator, $\hat{F}$ does not reach a peak.

The results in Figure 4 are difficult to compare because of the large differences in magnitude of the results. However, an alternative nondimensional plot allows better comparison. Consider comparing F with the force required to bend a bar in the lattice. For any bending deformation, the force applied for a displacement δ will be given by $(cEAk^2/l^2) \times (\delta/l)$, where c is a constant depending on the support condition. Thus the appropriate nondimensional form of F is

$$\frac{F}{EAk^2/l^2} = \frac{F}{EAs^2} = \frac{\hat{F}}{s^2}$$

and it is this form that we shall use for an alternative plotting of the results.

The values of $\hat{F}/s^2$ during actuation are shown in Figure 5, for the flexible actuator only. Note that the abscissa used here is ε_a/s — effectively measuring actuation displacements relative to the thickness, rather than the length, of the the bar. It was found in [Wicks and Guest 2004] that, for a kagome lattice, the nondimensional energy of actuation, or equivalently the nondimensional actuation stiffness, $d\hat{F}/d\varepsilon_a$ for small ε_a, was proportional to s [Leung et al. 2004]. Hence the choice of abscissa, ε_a/s, and the choice of ordinate, $\hat{F}/s^2$, ensures that the slope of the lines for $\varepsilon_a = 0$ is approximately equal for all s. These

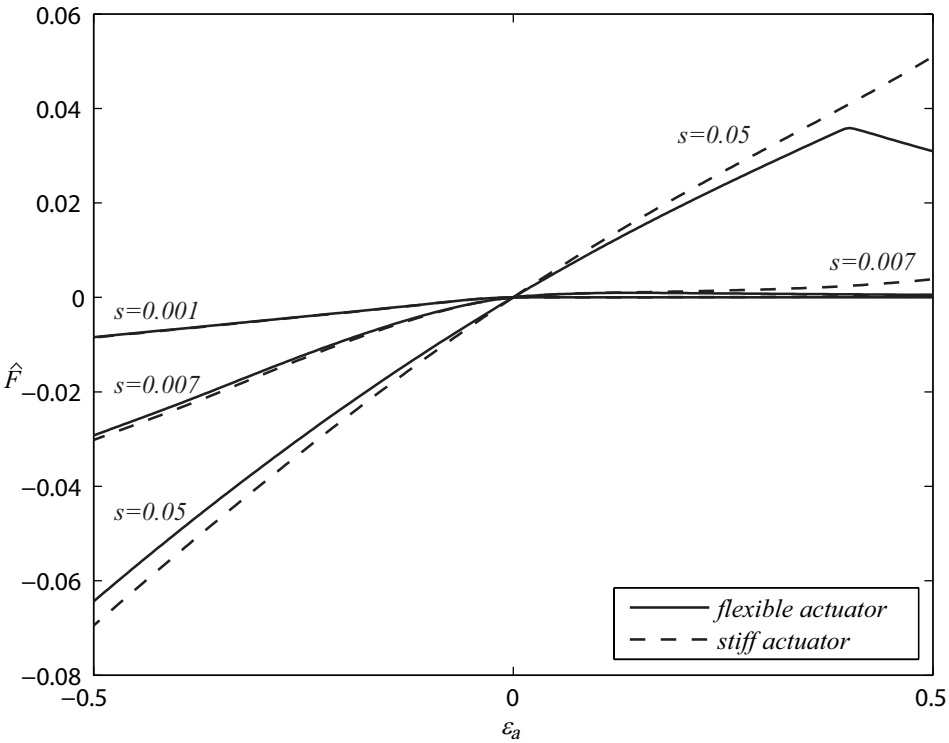

Figure 4. Nondimensional actuation force calculated using geometrically nonlinear models, for both flexible and stiff actuators, and $s = 0.001$, $s = 0.007$ and $s = 0.05$.

features can be seen in Figure 5. Note that in Figure 5, the maxima in $\hat{F}$ for $s = 0.001$ and $s = 0.007$ now occur outside the range of data plotted. Results for the stiff actuator in this range are rather similar (apart from the absence of the peak for $s = 0.05$) and are not shown for clarity.

5. Actuation limit

We consider two limiting cases for actuation. The first is when actuation is limited by the material properties of the lattice material: we consider the structure ineffective when a yielding strain is reached somewhere in the lattice. An alternative limit is when the actuator is not able to apply an increased force to the deform the rest of the lattice — either due to a classical buckling phenomenon, or because deformation has localised within the actuator.

5.1. ***Strain limited actuation.*** We consider limitation on the actuation of a structure that yielding anywhere in the structure outside of the actuator must be avoided. This section reports numerical results for the peak achievable actuation strain in infinite kagome lattices.

Flexible actuator. Figure 6 shows the magnitude of actuation strain, ε_a, at which first yield occurs plotted against stockiness, s, for a flexible actuator. Various values of material yield strain, ε_y, for both positive and negative actuation are included, covering a practical range of yield strains from material such as mild steel ($\varepsilon_y \approx 0.125\%$) to titanium ($\varepsilon_y \approx 2.0\%$). In each case, the yield strain is reached at some position in

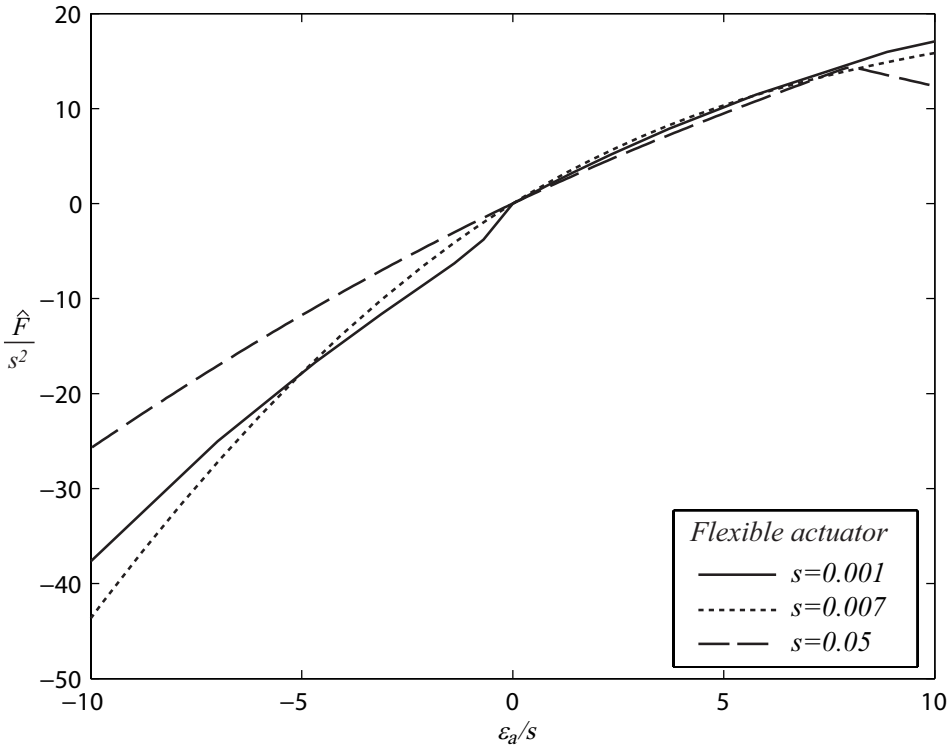

Figure 5. Nondimensional actuation force within the actuated bar plotted against the imposed strain, for only the flexible actuator, and stockiness $s = 0.001$, $s = 0.007$ and $s = 0.05$. Note this is the same data plotted in Figure 4, with different scaling.

the bar immediately adjacent to the actuator, as shown in Figure 8(a). The position of first yield varies with the stockiness of the lattice.

The results are shown only up to $\varepsilon_a = 0.5$ and are truncated by the line of peak actuation force, marked by crosses in Figure 6. Peak force achieved in a flexible actuator indicates a limit on the practicality of the kagome lattice as an active structure. Peak force occurs at an actuation strain proportional to the stockiness of the lattice: the results are also plotted in Figure 9 and discussed in Section 5.2.

The result from Figure 6 shows for smaller stockiness and higher yield strains, geometric nonlinearity affects maximum actuation strain most severely. For the smallest yield strain case $\varepsilon_y = 0.125\%$, it is observed that when stockiness decreases in the positive actuation case, peak actuation is suddenly lowered from the gradually increasing trend. The same effect is observed for other ε_y. In the negative actuation cases, no sudden drop in achievable actuation strain is observed.

Stiff actuator. Figure 7 shows the magnitude of actuation strain, ε_a, at which first yield occurs plotted against stockiness, s, for a stiff actuator. Three material yield strains, ε_y, from 0.125% to 2.0% are included, for both positive and negative actuation. In each case, the yield strain is reached at some position in the bar immediately adjacent the actuator, as shown in Figure 8(b). The position of first yield varies with the stockiness of the lattice.

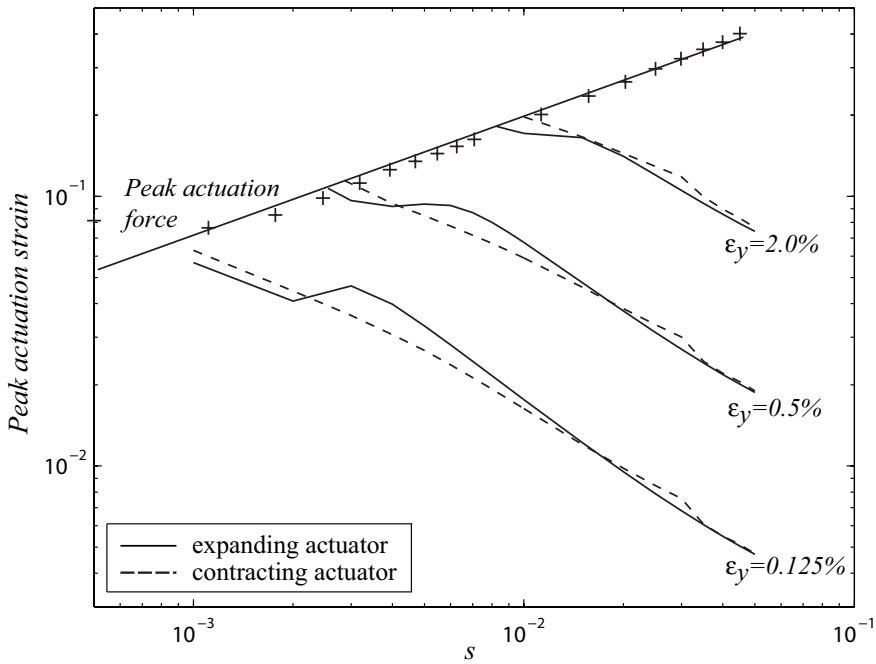

Figure 6. Peak actuation strain achievable for the flexible actuator before either the material yields, or a peak force is reached in the actuator.

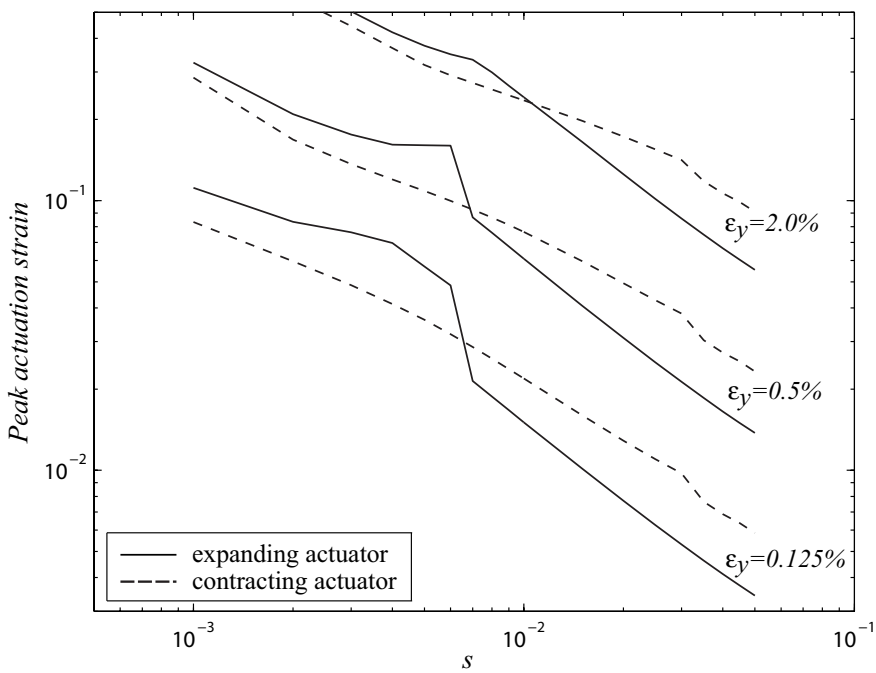

Figure 7. Peak actuation strain achievable for the stiff actuator before either the material yields, or a peak force is reached in the actuator.

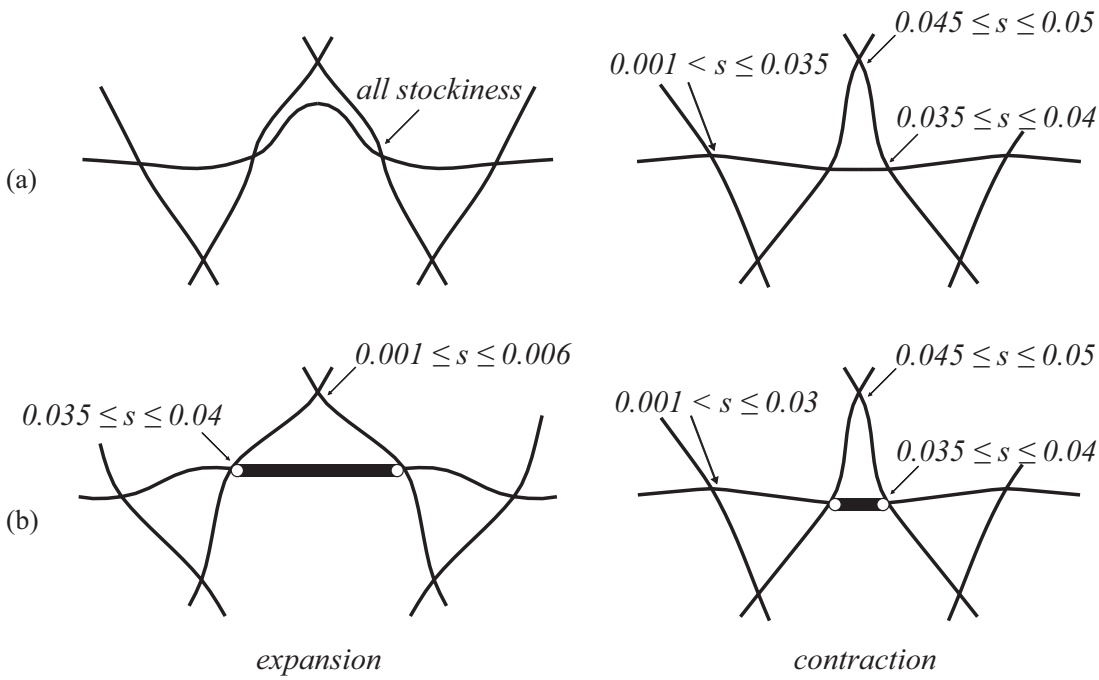

Figure 8. The position of the peak strain in the kagome lattice due to the actuation of a single bar, indicated by arrows, with (a) flexible, and (b) stiff actuation.

5.2. ***Peak actuation force and buckling.*** In Figure 6, the straight line marked by crosses shows the actuation strain at which peak actuation force in the actuator is achieved. This peaking effect can be seen in Figure 4 for $s = 0.05$: the solid line representing flexible positive actuation peaks at approximately $\varepsilon_a = 0.4$. This critical actuation strain exists for each of the models with a flexible actuator, and its value increases approximately linearly with the stockiness of the lattice. These data is also shown in Figure 9. When actuation force ceases to increase with actuation strain, the maximum activation capability of the lattice is reached. This phenomenon is only observed in the positive flexible actuation case, and we consider it as a limiting case of actuation of the kagome lattice.

One way to predict the peak actuation force would be to consider a bifurcation analysis based on a linear model. However, for this case, this is not found to give good results, as is shown in Figure 9: the structure undergoes large deformations before the peak force is obtained, and this renders a prediction based on a linear model inaccurate. Another possible failure mode is out-of-plane buckling, which is investigated in the following section.

5.3. ***Buckling of an imperfect structure .*** The results described thus far are for a perfect planar structure. For most practical uses of a kagome lattice, deformation out of plane is likely to be restrained [Santos e Lucato et al. 2004; Symons et al. 2005a; 2005b]. However, we do here consider the possible out-of-plane buckling by considering a full three-dimensional structure with imperfections. This has the useful side-effect of showing that the imperfections barely affect the in-plane response.

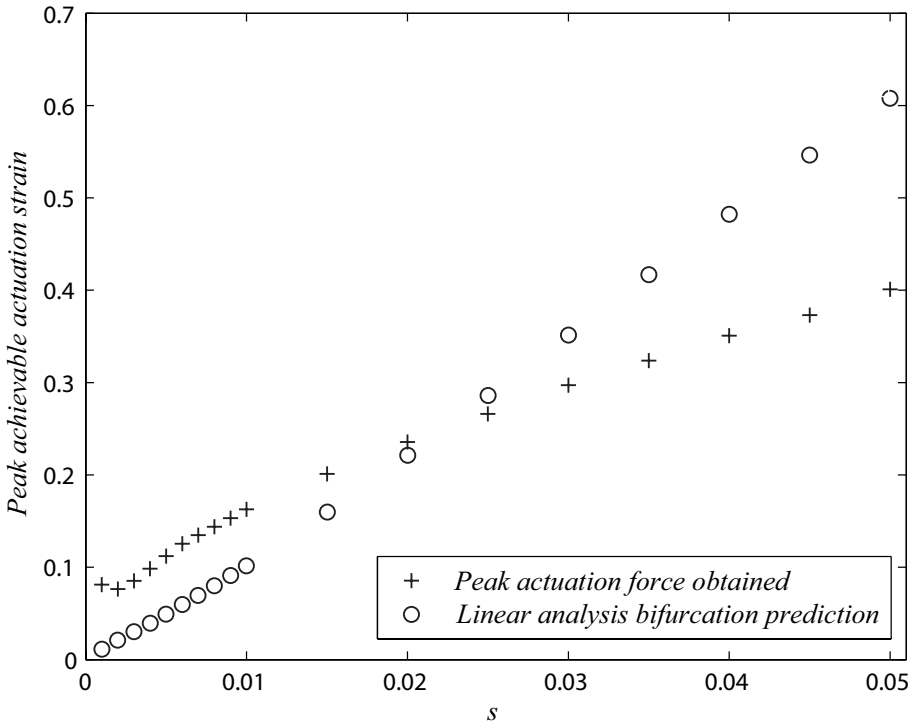

Figure 9. Comparison of limiting actuation strain at peak actuation force and buckling load.

Random imperfection has been implemented into the system to invoke any possible buckling modes. The magnitude of imperfection, δ, in a particular direction, is a function of radius of gyration, and is defined as

$$\delta_x, \delta_y, \delta_z = P * R * 2k,$$

where P is the imperfection factor: values of 0.01%, 0.1% and 1.0% were used. R is a normally distributed random number between 0 and ± 1.0; and k is the radius of gyration of the model. These imperfections are applied on all the member nodes of a kagome lattice model, except the actuator. Results show that no in-plane buckling response occurs. The in-plane response is indistinguishable from the 'perfect' results described in Section 4. Thus the following will focus on the effect of out-of-plane imperfections, δ_z, on the out-of-plane buckling response.

The response of the imperfect structure to actuation is plotted in Figure 10 for models with circular bars of $s = 0.01$ and flexible actuator, together with results for the perfect structure for comparison. The response of the imperfect structure initially matches that of the perfect structure, but at some point, depending on the imperfection factor, P, there is a sudden drop in the actuator load, and the structure deforms into a plate buckling like deformed mode. If the actuation is reversed for a buckled structure, the structure follows this post-buckling path, and does not return to the initial curve until the actuation reaches zero.

For cases when there is no out-of-plane restraint, the out-of-plane buckling can still be suppressed by increasing the out-of-plane bending stiffness of the bars. Models with rectangular cross-section bars have been analyzed, with constant imperfection factor and a flexible actuator. To maintain a constant s, the in-plane dimension, d, of the members must remain constant, while the out-of-plane dimension, b, is altered. Figure 11 shows results from changing b, while keeping, d, s and the imperfection factor constant; b ranges from $0.5d$ to $4d$. By increasing one dimension of the bar cross-section, the actuation response approaches that of the perfect model.

The results above have all been for a flexible actuator. Essentially similar results were obtained for a stiff actuator.

6. Discussion

It is found that positive actuation causes a decrease in actuation stiffness. This effect is especially prominent at small stockiness because of the smaller member bending stiffness. For flexible actuators only, $\hat{F}$ reaches a peak value.

Negative actuation results in an increased actuation stiffness, for both flexible and stiff actuation, indicating a stiffening response. This is due to a more stretching dominated response invoked by a contracting actuator.

The mode of deformation can provide explanation for the softening and stiffening effects under single-member actuation. The softening response observed with positive flexible actuation is caused by localised deformation within the actuator itself. Figure 3, top left, shows severe bending deformation in the flexible actuator when stockiness is low. It shows that deflection attenuation is exceptionally rapid for the smallest stockiness $s = 0.001$, where almost all deformation is found within the actuator and the colinear bars immediately adjacent. For positive stiff actuation, Figure 3, top right, shows a similar response where local deformation is concentrated near the actuator. As these bars deform quickly and locally with increasing actuation, less effective actuation can be transmitted to the rest of the structure.

Negative actuation causes deflection to propagate in a direction perpendicular to the actuator, especially when stockiness is small. In Figure 3, bottom middle, where actuation is small and linear, deflection is largely confined within the actuator's corridor. With large actuation, Figure 3, bottom left and right, shows that more diagonal bars are affected, and this contributes to the stiffening effect observed.

Figure 4 shows the discrepancies between flexible and stiff actuation models of the same stockiness. The sudden decrease in stiffness observed in flexible actuation models are not observed in the stiff actuation models. This shows that the peak in actuation force, described in the above discussion, is the result of the properties of the actuator deforming in bending. Kagome lattices can be made more effective for positive actuation if the actuator is stiffer.

Finally, actuation is limited only by material strength and the limitation on actuation force. In-plane buckling proves not to be an important consideration.

Appendix: Spring boundary stiffness derivation

The springs at the boundary of the modelled lattice should represent an infinite continuation of the kagome lattice. As long as the modelled lattice is large enough, the deformations at the boundary will be small, and hence the result of a linear model gives an appropriate boundary spring stiffness.

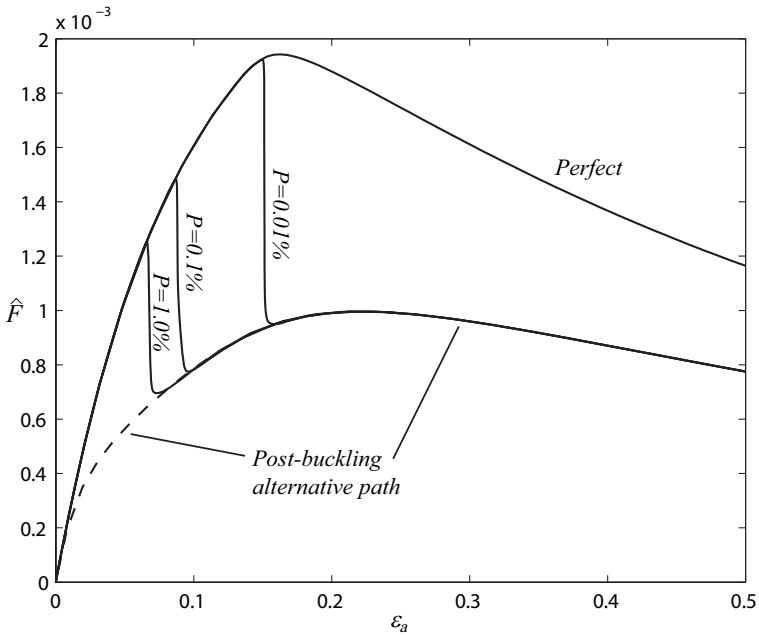

Figure 10. Actuation force versus actuation strain for kagome lattice models of $s = 0.01$ with a flexible actuator and circular bars. Results are shown for three imperfection factors, P. The dashed line indicates reverse loading. The 'perfect' result from 2D modeling is included for comparison.

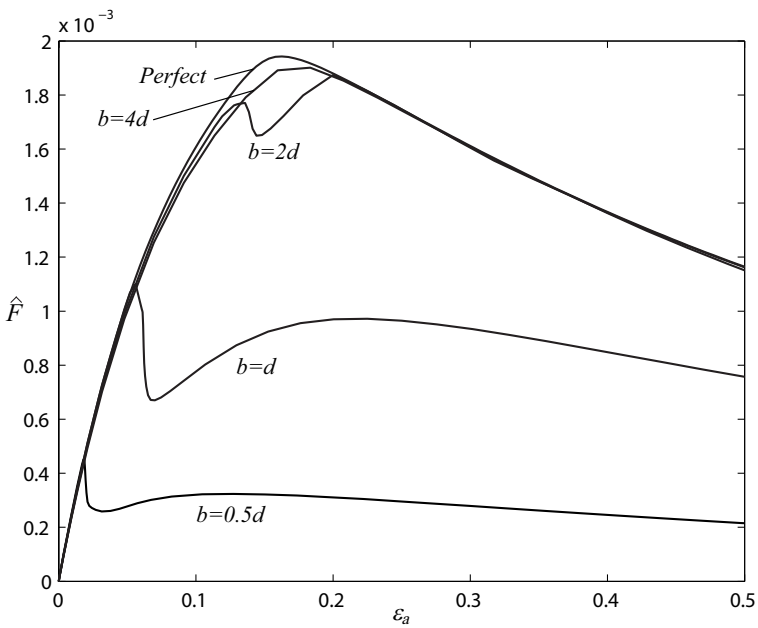

Figure 11. Actuation force versus actuation strain for kagome lattice models of $s = 0.01$ with a flexible actuator and rectangular bars. The in-plane dimension d is kept constant, and the out-of-plane dimension b varies. The 'perfect' result is included for comparison.

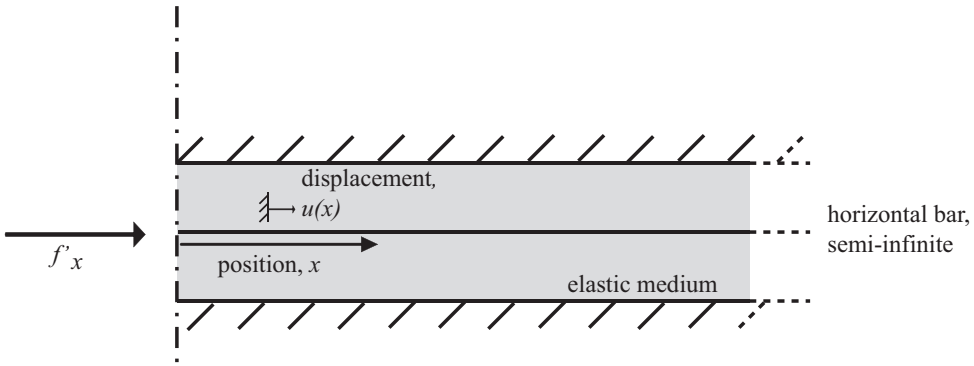

Figure 12. Smeared stiffness model, where a bar is suspended in an elastic material; adapted from [Wicks and Guest 2004].

Here, we adapt the smeared stiffness model shown in Figure 12 to find the boundary stiffness. Now the force f'_x represents the force at the edge of the modelled lattice. Wicks and Guest [2004] show that

$$u(x) = u_0 e^{-cx}, \tag{1}$$

where $u(x)$ is the horizontal nodal displacement of colinear bar members, u_0 is the displacement at $x = 0$, and a simple estimate gives $c = 4\sqrt{3}s/L$. If we consider that the central bar remains elastic, with axial stiffness AE and strain du/dx, its tension $t(x)$ is given by

$$t(x) = AE\frac{du}{dx} = -cAEu_0 e^{-cx},$$

so the central force f'_x is obtain from the tension at the $x = 0$ position:

$$f'_x = -t(0) = cAEu_0. \tag{2}$$

This response can be represented by a spring of stiffness k; combining (1) and (2) we get

$$k = \frac{f'_x}{u_0} = cAE = 4\sqrt{3}s\frac{AE}{L}.$$

In fact, this estimate can be improved by considering linear finite element models with a large range of stockiness, to give a more suitable accurate relationship, where $k_{\text{empirical}} = 0.6134k$. It was found that using boundary springs with this stiffness gave essentially identical results to those described in this paper with a modelled lattice that was either double or half the original model's width and height, showing that the boundary was correctly modelled.

References

[Akin 1986] J. E. Akin, *Finite element analysis for undergraduates*, Academic Press, London, 1986.

[Dean 1976] D. L. Dean, *Discrete field analysis of structural systems*, Springer, New York, 1976.

[Deshpande et al. 2001] V. S. Deshpande, M. F. Ashby, and N. A. Fleck, "Foam topology bending versus stretching dominated architectures", *Acta Mater.* **49**:6 (2001), 1035–1040.

[Hutchinson et al. 2003] R. G. Hutchinson, N. Wicks, A. G. Evans, N. A. Fleck, and J. W. Hutchinson, "Kagome plate structures for actuation", *Int. J. Solids Struct.* **40**:25 (2003), 6969–6980.

[Karpov et al. 2002] E. G. Karpov, D. L. Dorofeev, and N. G. Stephen, "Characteristic solutions for the statics of repetitive beam-like trusses", *Int. J. Mech. Sci.* **44**:7 (2002), 1363–1379.

[Leung et al. 2004] A. C. H. Leung, D. D. Symons, and S. D. Guest, "Actuation of kagome lattice structures", in *Proceedings of the 45th AIAA/ASME/ASCE/AHS/ASC Structures, Structural Dynamics and Materials Conference* (Palm Springs, CA), AIAA, Reston, VA, 2004. Paper #2004-1525.

[Noor 1998] A. K. Noor, "Contiunuum modelling for repetitive lattice structures", *Appl. Mech. Rev.* **41** (1998), 285–296.

[Noor and Zhang 2006] N. G. Noor and Y. Zhang, "Eigenanalysis and continuum modelling of pre-twisted repetitive beam-like structures", *Int. J. Solids Struct.* **43**:13 (2006), 3832–3855.

[Renton 1984] J. D. Renton, "The beam-like behaviour of space trusses", *AIAA J.* **22**:2 (1984), 273–280.

[Santos e Lucato et al. 2004] S. L. dos Santos e Lucato, J. Wang, P. Maxwell, R. M. McMeeking, and A. G. Evans, "Design and demonstration of a high authority shape morphing structure", *Int. J. Solids Struct.* **41**:13 (2004), 3521–3543.

[Symons et al. 2005a] D. D. Symons, R. G. Hutchinson, and N. A. Fleck, "Actuation of the kagome double-layer grid, 1: Prediction of performance of the perfect structure", *J. Mech. Phys. Solids* **53**:8 (2005), 1855–1874.

[Symons et al. 2005b] D. D. Symons, R. G. Hutchinson, and N. A. Fleck, "Actuation of the kagome double-layer grid, 2: Effect of imperfections on the measured and predicted actuation stiffness", *J. Mech. Phys. Solids* **53**:8 (2005), 1875–1891.

[Timoshenko and Gere 1961] S. P. Timoshenko and J. M. Gere, *Theory of elastic stability*, 2nd ed., McGraw-Hill, New York, 1961.

[Wicks and Guest 2004] N. Wicks and S. D. Guest, "Single member actuation in large repetitive truss structures", *Int. J. Solids Struct.* **41**:3–4 (2004), 965–978.

Received 28 Apr 2006. Accepted 5 Dec 2006.

ANTHONY C. H. LEUNG: anthony.leung@cantab.net
Department of Engineering, University of Cambridge, Trumpington Street, Cambridge CB2 1PZ, United Kingdom

SIMON D. GUEST: sdg@eng.cam.ac.uk
Department of Engineering, University of Cambridge, Trumpington Street, Cambridge CB2 1PZ, United Kingdom
http://www.eng.cam.ac.uk/~sdg